# Kinetic study of ion acoustic twisted waves with kappa distributed electrons

Kashif Arshad, Aman-ur-Rehman, and Shahzad Mahmood

Citation: Physics of Plasmas **23**, 052107 (2016); doi: 10.1063/1.4947555
View online: http://dx.doi.org/10.1063/1.4947555
View Table of Contents: http://scitation.aip.org/content/aip/journal/pop/23/5?ver=pdfcov
Published by the AIP Publishing



# Kinetic study of ion acoustic twisted waves with kappa distributed electrons

Kashif Arshad,[1,a)] Aman-ur-Rehman,[1,b)] and Shahzad Mahmood[1,2,c)]
[1]*Pakistan Institute of Engineering and Applied Sciences, P. O. Nilore, Islamabad 45650, Pakistan*
[2]*Theoretical Physics Division, PINSTECH P.O. Nilore, Islamabad 44000, Pakistan*

(Received 10 January 2016; accepted 11 April 2016; published online 9 May 2016)

The kinetic theory of Landau damping of ion acoustic twisted modes is developed in the presence of orbital angular momentum of the helical (twisted) electric field in plasmas with kappa distributed electrons and Maxwellian ions. The perturbed distribution function and helical electric field are considered to be decomposed by Laguerre-Gaussian mode function defined in cylindrical geometry. The Vlasov-Poisson equation is obtained and solved analytically to obtain the weak damping rates of the ion acoustic twisted waves in a non-thermal plasma. The strong damping effects of ion acoustic twisted waves at low values of temperature ratio of electrons and ions are also obtained by using exact numerical method and illustrated graphically, where the weak damping wave theory fails to explain the phenomenon properly. The obtained results of Landau damping rates of the twisted ion acoustic wave are discussed at different values of azimuthal wave number and non-thermal parameter kappa for electrons. *Published by AIP Publishing.*
[http://dx.doi.org/10.1063/1.4947555]

## I. INTRODUCTION

In this modern age, electromagnetic (EM) fields have various applications in fundamental research, communication, and home appliances. Even though, there are still some subtle features of electromagnetic field known to us a century ago,[1] yet to be utilized. It is because of the technical complexities to sense three dimensional (3D) electromagnetic field. An important characteristic of electromagnetic field is its orbital angular momentum (OAM),[2–5] used in modern experiments that involve trapping of atoms, molecules, and microscopic particles[6] using laser fields and interaction between photon and atmospheric turbulence.[7] The orbital angular momentum (OAM) is mostly used in optical frequency range[8] for fast encoding of information in free space communication but not fully in the radio frequency range. Now scientists are interested in studying the effect of orbital angular momentum (OAM) in other research areas like radio waves[9] and modern radio telescopes like the Low Frequency Array (LOFAR) or European Incoherent Scatter (EISCAT) ionospheric radar facility to observe 3D plasma dynamics in the ionosphere or Lunar Infrastructure for Exploration (LIFE),[10] inverse Faraday effect,[11] neutrino physics,[12] and plasmas.[13]

For many years, the characteristics of one form of electromagnetic radiation, such as laser beams, have been studied in optics. These Laser beams consist of distinct laser modes.[14] The most common of laser modes is the Hermite-Gaussian (HG) modes but other modes like Laguerre-Gaussain (LG) and Bessel-Gaussain (BL) modes may exist in smaller amounts. Using suitable optical devices, the Hermite-Gaussian (HG) beams can be converted into Laguerre-Gaussain (LG) modes.[15] The Laguerre-Gaussain (LG) modes exhibit characteristic orbital angular momentum.[16] The ring shape morphology of a beam with orbital angular momentum (OAM) is ideal for the observation of solar corona around the sun where the intensity of the beam is minimum at the center, in solar experiments,[17] astrophysical environment,[18] and earth's ionosphere.[19]

In recent years, stimulated scattering instabilities are investigated in dense quantum (degenerate electron-non-degenerate ion) plasma for the coherent circularly polarized electromagnetic (CPEM) waves carrying orbital angular momentum.[20] The three dimensional modified kinetic Alfvén wave (3D m-KAW) is estimated using Ampere's law and two fluid model in a magnetized plasma, which are outcome of plasma density whirls or magnetic flux ropes with orbital angular momentum. These 3D m-KAWs are termed as Alfvénic tornadoes[21] and have solution like Laguerre-Gaussian Alfvénic vortex beam in the presence of plasma density whirls. Some certain scattering phenomenon like (stimulated Raman and Brillouin backscattering) is observed to be responsible for the interaction between electrostatic and electromagnetic waves through orbital angular momentum.[22] The trapping and transport of dust particles are predicted with the twisted dust acoustic (DA) vortex beam.[23] The twisted electrostatic and electromagnetic plasma modes are supposed to exhibit special characteristics in the presence of orbital angular momentum.[24] Shukla obtained the dispersive shear Alfvén wave (DSAW) modes from generalized ion vorticity and electron momentum equations aligned with the magnetic field[25] in a magnetized plasma. These modes are capable of trapping and transport of particles in Earth's auroral zone, in the solar atmosphere, and in Large Plasma Device (LAPD) at University of California, Los Angeles.

Leyser[26] studied experimentally the creation and pumping of radio beam with helical wave front carrying OAM into the ionospheric plasma under High frequency Active

[a)]kashif.arshad.butt@gmail.com
[b)]amansadiq@gmail.com
[c)]shahzadm100@gmail.com

Auroral Research Program (HAARP). The optical emission spectrum of pumped plasma turbulence shows the characteristics of ring shaped morphology due to pumped twisted radio beam. In further studies, the braided electrostatic ion cyclotron (ESIC) modes are predicted in Saturn's F-ring[27] in a dusty magnetoplasma. Such modes have ability to trap and transport particles in a magnetized plasma. When solar wind excites the 3D kinetic Alfvén wave (KAW), the wave grows as modulational instability[28] in the form of a vortex beam, which confirms the presence of OAM of wave eigen modes.

The kinetic theory for the twisted electron modes[29] and ion acoustic plasma vortices[30] has been developed by considering Maxwellian distribution. These waves could be excited by nonlinear decay of laser beams with orbital angular momentum (OAM) or rotating electron beams. These complex helical wave structures develop new features of the Landau resonance and instabilities. But most of the space plasmas and in some laboratory experiments the charged particles have shown non-Maxwellian or non-thermal distribution of particles.[31–33] These non-thermal charged particles in most of the cases are electrons that can be described well by using generalized Lorentzian or kappa (non-Maxwellian) distribution function.[34]

In this manuscript, kinetic theory is applied to study the ion acoustic waves in the presence of electric field carrying orbital angular momentum in a plasma containing Maxwellian ions and non-Maxwellian electrons described by the Maxwellian and generalized Lorentzian or kappa distribution functions. The manuscript is composed of various sections. Section II contains basic set of equations (Vlasov equation, Poisson equation, and paraxial equation) for the twisted ion acoustic waves. In Section III, the modified plasma dispersion function with electric field having orbital angular momentum is derived for kappa distributed electrons and Maxwellian distributed ions by decomposing the potential and distribution function in Laguerre-Gaussian (LG) modes. By using the modified dispersion function, the dielectric function of twisted ion acoustic wave in plasmas with nonthermal electrons and thermal ions and the weak Landau damping rates of the wave are calculated analytically. In Section IV, the numerical plots for weak Landau damping rates and exact numerical solution for strong Landau damping effects by using Newton Raphson method are illustrated. Finally, the conclusion is presented in the same section.

## II. THEORETICAL MODEL

In this section, we will present the basic equations to describe the kinetic theory of ion acoustic wave acquiring some specific orbital angular momentum. The distribution function $f_\alpha(\mathbf{r},\mathbf{v},t)$ can be obtained from the well known Vlasov equation, where $\alpha = e$ $(i)$ for the electrons (ions). By applying the perturbation analysis, the distribution function $f_\alpha(\mathbf{r},\mathbf{v},t)$ of the ion acoustic waves splits into two parts, a perturbed part $\hat{f}_\alpha$ and a background part $f_{\alpha 0}$ given by the expression $f_\alpha = f_{\alpha_0} + \hat{f}_\alpha$. Now, we will perform linearization on the Vlasov equation with respect to perturbation, which gives us

$$\left(\frac{\partial}{\partial t} + \mathbf{v}\cdot\frac{\partial}{\partial \mathbf{r}}\right)\hat{f}_\alpha - q_\alpha \mathbf{E}\cdot\frac{\partial}{\partial \mathbf{p}_\alpha} f_{\alpha 0} = 0. \tag{1}$$

Here $\mathbf{p}_\alpha$ represents the momentum such that $\mathbf{p}_\alpha = m_\alpha \mathbf{v}$ and $\mathbf{E}$ is the electric field $\mathbf{E} = -\nabla\phi$. The electric field can be calculated from the linearized Poisson equation given below

$$\nabla^2\phi = 4\pi \sum_{\alpha=e,i} q_\alpha \int \hat{f}_\alpha(\mathbf{v}) d\mathbf{v}. \tag{2}$$

Consider the propagation of the ion acoustic plasma wave with slowly varying amplitude along the z-axis, i.e., $exp(ikz)$, such that

$$\nabla^2\phi = (\partial_\perp^2 - k^2 + 2ik\partial_z)\phi. \tag{3}$$

Here, the transverse Laplacian operator $\partial_\perp^2$ is written as $\partial_\perp^2 = (1/r)\partial/\partial r(r\partial/\partial r) + (1/r^2)\partial^2/\partial\theta^2$ in cylindrical coordinate system. The field gradually varies along the z-axis such that $\partial_z^2\phi \ll 2k\partial_z\phi$. Under these conditions, the wave has a finite orbital angular momentum corresponding to the potential $\phi$ and they satisfy the paraxial equation given by

$$(\partial_\perp^2 + 2ik\partial_z)\phi = 0. \tag{4}$$

The existence of these waves is such that they must satisfy the Poisson equation (2) which gives

$$-k^2\phi = 4\pi \sum_{\alpha=e,i} q_\alpha \int \hat{f}_\alpha(\mathbf{v}) d\mathbf{v}. \tag{5}$$

Here, $q_e = -e$ and $q_i = e$ (where $-e$ is the electronic charge). Equations (1)–(5) are the basis of the ion acoustic plasma waves with orbital angular momentum of the electric field.

## III. PLASMA DISPERSION FUNCTION WITH HELICAL ELECTRIC FIELD

We will consider the solutions of paraxial equation Eq. (4) for the calculation of modified plasma dispersion function in the presence of orbital angular momentum. These solutions can be obtained by the superposition of Laguerre-Gaussian (LG) functions described in cylindrical coordinate system $\mathbf{r} = (r,\theta,z)$. By definition of Laguerre-Gaussian (LG) function $F_{pl}(r,z)$ (which is described in Ref. 34 with its properties as well), the potential $\phi(\mathbf{r},t)$ can be written as follows:

$$\phi(\mathbf{r},t) = \sum_{pl} \tilde{\phi}_{pl} F_{pl}(r,z) e^{i\theta} e^{ikz - i\omega t}. \tag{6}$$

Here, $\tilde{\phi}_{pl}$ is the mode amplitude and integers $p$ and $l$ are the radial and angular mode numbers, while $\theta$ denotes the azimuthal angle. Using spatial structure of given potential described in Eq. (6), the helical electric field can be written in terms of $k_{eff}$ (effective wave number) as $\mathbf{E} = -i\mathbf{k}_{eff}\phi$, where $k_{eff}$ is defined by the following expression:

$$\mathbf{k}_{eff} = -\frac{i}{F_{pl}}\partial_r F_{pl}\mathbf{e}_r + \frac{l}{r}\mathbf{e}_\theta + \left(k - \frac{i}{F_{pl}}\partial_z F_{pl}\right)\mathbf{e}_z. \quad (7)$$

Therefore, the helical electric field can also be resolved into its components as follows:

$$E_r = -\frac{\partial\phi}{\partial r} = -\frac{i}{F_{pl}}\partial_r F_{pl}, \quad (8)$$

$$E_\theta = -\frac{l}{r}\frac{\partial\phi}{\partial\theta} = -\frac{il}{r}\phi, \quad (9)$$

and

$$E_z = -\frac{\partial\phi}{\partial z} = -\left(ik + \frac{1}{F_{pl}}\partial_z F_{pl}\right)\phi. \quad (10)$$

The above set of Equations (8)–(10) confirms that the electric field exhibits helical structures instead of straight lines (as in case of ordinary plane wave solutions) along the z-direction. But in accordance with the paraxial approximation, the axial component of the electric field is still dominant.

In order to obtain the solution of coupled Vlasov-Poisson equations ((1) and (5)), we will decompose the perturbed distribution function in Laguerre-Gaussian (LG) modes such that

$$\tilde{f}_\alpha(\mathbf{v}) = \sum_{pl}\tilde{f}_{pl}(\mathbf{v})F_{pl}(r,z)e^{il\theta}e^{ikz-i\omega t}. \quad (11)$$

Further, we will substitute the decomposed distribution function (11) into the standard Vlasov equation (1). The resultant equation is then multiplied by $F_{pl}$ and integrated in $rdr$ with orthogonality condition described in Ref. 34. After applying the orthogonality condition, the final form of resultant equation is given as

$$\tilde{f}_{pl} = \sum_{\alpha=e,i}\frac{q_\alpha}{m_\alpha}\frac{\tilde{\phi}_{pl}}{(x+iy)}\left(\mathbf{q}_{eff}\cdot\partial_{\mathbf{v}}f_{\alpha 0}\right). \quad (12)$$

Here, $x$ and $y$ can be defined as

$$x = (\omega - kv_z) - lq_\theta v_\theta, \qquad y = (q_r v_r + q_z v_z), \quad (13)$$

such that $x + iy = (\omega - \mathbf{q}_{eff}\cdot\mathbf{v})$ and

$$\mathbf{q}_{eff} = -iq_r\hat{\mathbf{e}}_r + lq_\theta\hat{\mathbf{e}}_\theta + (k - iq_z)\hat{\mathbf{e}}_z. \quad (14)$$

Here, the parameters $q_j$ and $q_\theta$ are defined as

$$q_j = \int_0^\infty F_{pl}\partial_j F_{pl} r dr \text{ where } (j = r,z), \quad q_\theta = \int_0^\infty F_{pl}^2 dr. \quad (15)$$

We will now use the value of decomposed perturbed distribution function $\tilde{f}_{pl}$ from (12) into the Poisson equation (5), to get the general form of plasma dielectric function. We can write the plasma dielectric function $\epsilon(\omega,k,lq_\theta)$ for the twisted ion acoustic waves in the presence of kappa distributed (non-thermal) electrons as follows:

$$\epsilon(\omega,k,lq_\theta) = 1 + \sum_{\alpha=e,i}\frac{\omega_{p\alpha}^2}{k^2}\int\frac{\mathbf{q}_{eff}\cdot\partial_{\mathbf{v}}f_{0\alpha}}{(\omega - \mathbf{q}_{eff}\cdot\mathbf{v})}d\mathbf{v}, \quad (16)$$

where $\chi(\omega,k,lq_\theta)$ is the susceptibility of electron-ion plasma which is defined as

$$\chi(\omega,k,lq_\theta) = \sum_{\alpha=e,i}\frac{\omega_{p\alpha}^2}{k^2}\int\frac{\mathbf{q}_{eff}\cdot\partial_{\mathbf{v}}f_{0\alpha}}{(\omega - \mathbf{q}_{eff}\cdot\mathbf{v})}d\mathbf{v}.$$

Here, $\omega_{p\alpha} = \sqrt{4\pi n_{\alpha 0}^2 q_\alpha^2/m_\alpha}$ is the plasma frequency of the $\alpha$ specie. It can be written as

$$\epsilon(\omega,k,lq_\theta) = 1 + \chi_e(\omega,lq_\theta,k) + \chi_i(\omega,lq_\theta,k). \quad (17)$$

The above form of dielectric function in Equation (17) is similar to those for the usual dielectric function with planar electric field perturbations with an additional factor of azimuthal wave number $lq_\theta$ that appears due to the presence of orbital angular momentum of the electric field. From Eq. (16), we can write the modified condition of the Landau resonance in the presence of helical (twisted) electric field in comparison with planar electric field case as follows:

$$\omega = kv_z + lq_\theta v_\theta \pm i(q_r v_r + q_z v_z). \quad (18)$$

The imaginary part $y = (q_r v_r + q_z v_z)$ can be neglected for understanding the physical meaning of modified resonance condition, which is valid only if $|q_r|, |q_z| \ll |q_\theta|$ is satisfied. The modified resonance condition $\omega = kv_z + lq_\theta v_\theta$ resembles the Landau cyclotron resonance for the magneto plasma case.[35]

The susceptibility of electron-ion plasma carrying orbital angular momentum can be written in more simplified form as

$$\chi(\omega,lq_\theta,k) = \frac{\omega_{pe}^2}{k^2}Z_{\kappa,lq_\theta}(\xi_{ze},\xi_{\theta e}) + \frac{\omega_{pi}^2}{k^2}Z_{\kappa,lq_\theta}(\xi_{zi},\xi_{\theta i}), \quad (19)$$

where $Z_{\kappa,lq_\theta}(\xi_{ze},\xi_{\theta e})$ is the modified plasma dispersion function for electron (kappa distributed) and $Z_{\kappa,lq_\theta}(\xi_{zi},\xi_{\theta i})$ ion (Maxwellian distributed) plasmas with orbital angular momentum of the helical electric field is defined as

$$Z_{\kappa,lq_\theta}(\xi_{z\alpha},\xi_{\theta\alpha}) = \sum_{\alpha=e,i}\int\left[\frac{1}{u_z - v_z}\frac{\partial f_{0\alpha}}{\partial v_z}dv_z + \frac{1}{u_\theta - v_\theta}\frac{\partial f_{0\alpha}}{\partial v_\theta}dv_\theta\right]. \quad (20)$$

Here $\xi_z = u_z/\theta_\parallel$ and $\xi_\theta = u_\theta/\theta_\parallel$, where $u_z = \left(\frac{\omega}{k} - \frac{lq_\theta v_\theta}{k}\right)$ and $u_\theta = \left(\frac{\omega}{lq_\theta} - \frac{kv_z}{lq_\theta}\right)$.

Equation (17) can be written in terms of plasma dispersion function as follows:

$$\epsilon(\omega,k,lq_\theta) = 1 + \frac{\omega_{pe}^2}{k^2}Z_{\kappa,lq_\theta}(\xi_{ze},\xi_{\theta e}) + \frac{\omega_{pi}^2}{k^2}Z_{\kappa,lq_\theta}(\xi_{zi},\xi_{\theta i}). \quad (21)$$

The three dimensional non-Maxwellian (kappa) distributed electrons are given by the expression[34]

$$f_{0e}=\frac{n_{0_e}}{\pi^{3/2}\theta_\perp^2\theta_\parallel}\frac{\Gamma(\kappa+1)}{\kappa^{3/2}\Gamma(\kappa-1/2)}\left[1+\frac{v_\parallel^2}{\kappa\theta_{\parallel e}^2}+\frac{v_\perp^2}{\kappa\theta_{\perp e}^2}\right]^{-\kappa-1}, \quad (22)$$

where $\kappa$ is the spectral index and $\theta_{(\parallel,\perp)e}=\sqrt{(2\kappa-3)/\kappa}\times v_{T_e(\parallel,\perp)}$ with $\kappa>3/2$ is the effective thermal velocity for non-thermal electrons such that $v_{T_e(\parallel,\perp)}=\sqrt{T_{e(\parallel,\perp)}/m_e}$ is the thermal velocity of the electrons along the parallel and perpendicular directions, respectively. Here, $T_{e(\parallel,\perp)}$ is the electron temperature in energy units. The ions are comparatively massive and usually follow the three dimensional Maxwellian distribution as given by the equation:[35]

$$f_{0i}=\frac{n_{0i}}{(2\pi)^{3/2}v_{T_{\parallel i}}^2 v_{T_{\perp i}}}\exp\left(-\frac{v_\parallel^2}{v_{T_{\parallel i}}^2}+\frac{v_\perp^2}{v_{T_{\perp i}}^2}\right), \quad (23)$$

where $T_{i(\parallel,\perp)}$ is the ion temperature in energy units and $v_{T_i(\parallel,\perp)}=\sqrt{T_{i(\parallel,\perp)}/m_i}$ is the thermal velocity of ions in the parallel and perpendicular directions, respectively. The dispersion functions of the ion acoustic plasma waves in Eq. (21) with helical perturbed electric field, Lorentzian electrons, and Maxwellian distributed ions can be expanded under the condition ($\xi_{\theta i},\ \xi_{zi}\gg 1$ and $\xi_{\theta e},\ \xi_{ze}\ll 1$) obtained as follows:

$$\epsilon(\omega,k,lq_\theta)=1+\chi_e+\chi_i, \quad (24)$$

such that

$$\chi_e=\frac{1}{k^2\lambda_{De}^2}\frac{(\kappa-1/2)}{(\kappa-3/2)}-\frac{1}{\Upsilon^2}\frac{1}{k^2\lambda_{De}^2}+2i\sqrt{\pi}\frac{\omega\Gamma(\kappa+1)}{\kappa^{3/2}\Gamma(\kappa-1/2)}\times\frac{\omega_{pe}^2}{k^3\theta_{\parallel e}^3}\left[1+\Upsilon\left(1+\Upsilon^2\frac{\omega^2}{\kappa k^2\theta_{\parallel_e}^2}\right)^{-\kappa-1}\right],$$

and

$$\chi_i=-\frac{\omega_{pi}^2}{\omega^2}\left[1+\frac{3k^2v_{T_{\parallel i}}^2}{\omega^2}\right]-\frac{\omega_{pi}^2}{\Upsilon^2\omega^2}\left[1+\frac{3k^2v_{T_{\parallel i}}^2}{\Upsilon^2\omega^2}\right]+2i\sqrt{\pi}\frac{\omega\omega_{pi}^2}{k^3v_{T_{\parallel i}}^3}\left[\exp\left(-\frac{\omega^2}{2k^2v_{T_{\parallel i}}^2}\right)+\Upsilon\exp\left(-\Upsilon^2\frac{\omega^2}{2k^2v_{T_{\parallel i}}^2}\right)\right],$$

where $\Upsilon=k/lq_\theta$.

The dielectric function $\epsilon(\omega,k,lq_\theta)$ consists of real $Re[\epsilon(\omega,k,lq_\theta)]$ and imaginary $\mathrm{Im}[\epsilon(\omega,k,lq_\theta)]$ parts such that $\epsilon(\omega,k,lq_\theta)=Re[\epsilon(\omega,k,lq_\theta)]+\mathrm{Im}[\epsilon(\omega,k,lq_\theta)]$ and temporal angular velocity of the wave as $\omega=\omega_r+i\gamma$. The real part $\omega_r$ of the temporal angular frequency of the given twisted ion acoustic wave can be calculated by putting the real part of the dielectric function $\epsilon(\omega,k,lq_\theta)$ to zero which yields

$$\omega_r^2=\frac{k^2C_s^2}{\Upsilon^2}\left[\frac{(1+\Upsilon^2)}{\left(2\frac{(\kappa-1/2)}{(\kappa-3/2)}+k^2\lambda_{De}^2\right)}+\frac{3T_i}{T_e}\frac{(1+\Upsilon^4)}{(1+\Upsilon^2)}\right]. \quad (25)$$

The above equation presents the dispersion relation of twisted ion acoustic in the presence of Lorentzian electrons and Maxwellian distributed ions and $T_{\parallel e,i}=T_{e,i}$ has been defined in the further calculation. Here, we can define a new type of ion acoustic speed $C_{s,\mu}=C_{s_{OAM}}=C_s/\Upsilon$ (or twisted ion acoustic speed) with $C_s=\sqrt{T_e/m_i}$ known as acoustic speed for planar perturbations, and Eq. (25) is modified as follows:

$$\omega_r^2=k^2C_{s_{OAM}}^2\left[\frac{(1+\Upsilon^2)}{\left(2\frac{(\kappa-1/2)}{(\kappa-3/2)}+k^2\lambda_{De}^2\right)}+\frac{3T_i}{T_e}\frac{(1+\Upsilon^4)}{(1+\Upsilon^2)}\right]. \quad (26)$$

In the limit $\kappa\to\infty$, kappa distributed electrons exhibit Maxwellian distribution in the phase space and the above dispersion relation in Eq. (25) becomes the similar to that written in Eq. (24) of Ref. 30.

The weak Landau damping rate $\gamma$ for ion acoustic plasma waves with kappa distributed electrons in the presence of twisted electric field can be obtained from the relation $\gamma=-[\mathrm{Im}(\epsilon)/(\partial\mathrm{Re}(\epsilon)/\partial\omega)]_{\omega=\omega_r}$. Using the respective values of $\mathrm{Im}(\epsilon)$ and $\mathrm{Re}(\epsilon)$ in the expression of $\gamma$, we have

$$\gamma=-\frac{\sqrt{\pi}\omega_r^4\Upsilon^2}{k^2\omega_{pi}^2(1+\Upsilon^2)}[\gamma_e+\gamma_i], \quad (27)$$

where $\gamma_e$ and $\gamma_i$ are presenting the contributions of the electrons and the ions to the damping factor with expressions

$$\gamma_e=\frac{\Gamma(\kappa+1)}{\kappa^{3/2}\Gamma(\kappa-1/2)}\frac{\omega_r}{k}\frac{\omega_{pe}^2}{\theta_{\parallel e}^3}\left[1+\Upsilon\left(1+\Upsilon^2\frac{\omega_r^2}{\kappa k^2\theta_{\parallel_e}^2}\right)^{-\kappa-1}\right], \quad (28)$$

and

$$\gamma_i=\frac{\omega_r}{k}\frac{\omega_{pi}^2}{v_{T_{\parallel i}}^3}\left[\exp\left(-\frac{\omega_r^2}{2k^2v_{T_{\parallel i}}^2}\right)+\Upsilon\exp\left(-\Upsilon^2\frac{\omega_r^2}{2k^2v_{T_{\parallel i}}^2}\right)\right]. \quad (29)$$

In the limit, the azimuthal wave number approaches to zero, i.e., $lq_\theta\to 0$ or $\Upsilon\to\infty$; we will obtain the same results as that of the plane wave electric field perturbations. To understand it, we have to analyze the terms containing $\Upsilon$ in Eqs. (27)–(29). For $\Upsilon\to\infty$, the power term in Eq. (28) and exponential term in Eq. (29) decay very fastly to zero, which results in the vanishing of second term from $\gamma_e$ and $\gamma_i$ (i.e., damping due to twisted factor) from respective equations. Also in the limit $\Upsilon\to\infty$, the term $\Upsilon^2/(1+\Upsilon^2)=1$ in Eq. (27) gives the planar damping rate of the ion acoustic wave as follows:

$$\gamma=-\frac{\sqrt{\pi}\omega_r^4}{k^3\omega_{pi}^2}\left[\frac{\Gamma(\kappa+1)}{\kappa^{3/2}\Gamma(\kappa-1/2)}\frac{\omega_{pe}^2}{\theta_{\parallel e}^3}+\frac{\omega_{pi}^2}{v_{T_{\parallel i}}^3}\exp\left(-\frac{\omega_r^2}{2k^2v_{T_{\parallel i}}^2}\right)\right]. \quad (30)$$

From Equation (27), we get the following dimensionless weak damping rate of the ion acoustic twisted waves with Maxwellian distributed ions and kappa distributed electrons given by:

$$\frac{\gamma}{\omega_r} = -\frac{\sqrt{\pi}(1+\Upsilon^2)^{1/2}}{\Upsilon\left(2\frac{(\kappa-1/2)}{(\kappa-3/2)}+k^2\lambda_{De}^2\right)^{3/2}}\left[\sqrt{\frac{m_e}{m_i}}\gamma_e+\gamma_i\right], \quad (31)$$

and the simplified form of $\gamma_e$ and $\gamma_i$ is as follows:

$$\gamma_e = \frac{\Gamma(\kappa+1)}{(2\kappa-3)^{3/2}\Gamma(\kappa-1/2)} \times\left[1+\Upsilon\left(1+\frac{m_e/m_i}{(2\kappa-3)\theta_{\|_e}^2}\frac{(1+\Upsilon^2)}{\left(2\frac{(\kappa-1/2)}{(\kappa-3/2)}+k^2\lambda_{De}^2\right)}\right)^{-\kappa-1}\right], \quad (32)$$

and

$$\gamma_i = \left(\frac{T_e}{T_i}\right)^{3/2}\left[\exp\left(-\frac{1}{\Upsilon^2}\frac{T_e}{T_i}\frac{(1+\Upsilon^2)}{\left(2\frac{(\kappa-1/2)}{(\kappa-3/2)}+k^2\lambda_{De}^2\right)}\right) +\Upsilon\exp\left(-\frac{T_e}{T_i}\frac{(1+\Upsilon^2)}{\left(2\frac{(\kappa-1/2)}{(\kappa-3/2)}+k^2\lambda_{De}^2\right)}\right)\right]. \quad (33)$$

In the limit $\Upsilon = k/lq_\theta$ (ratio of parallel to azimuthal wave number) and spectral index kappa $\kappa$ approaches to infinity such that $\Upsilon \to \infty$ and $\kappa \to \infty$, the obtained Landau damping rate described in Eq. (31) with (32) and (33) is analogous to that given in Ref. 35.

## IV. NUMERICAL PLOTS

In this section, the weak and strong damping rates of the twisted ion acoustic wave vs $\beta = T_e/T_i$ (i.e., temperature ratio of electrons to ions) in plasma containing non-thermal kappa distributed electrons and Maxwellian distributed ions plasma are plotted. The weak damping rate of the wave is obtained from Eq. (31) with (32) and (33), respectively. However, the plots for strong damping rates of the ion acoustic twisted waves in non-thermal electrons plasma are obtained from the exact numerical solutions of Eq. (21) by putting $\epsilon(\omega, k, lq_\theta) = 0$. In order to find the imaginary roots (or damping roots) of the wave frequency from Eq. (21), the well known numerical technique (Newton Raphson method)[36] has been used. The obtained results are discussed below:

Figures 1(a) and 1(b) provide the analytical and exact numerical plots of normalized Landau damping rates $\gamma/\omega_r$ against $\beta = T_e/T_i$ (the temperature ratio of electrons to ions) of the twisted ion acoustic waves at various values of the azimuthal wave number $lq_\theta$ for the Maxwellian distributed electrons, i.e., $\kappa \to \infty$ case. Here, we have considered three cases of $\Upsilon = k/lq_\theta$ (ratio of parallel to azimuthal wave number) to plot the normalized damping rate of the wave vs $\beta$, i.e., (i) for the azimuthal wave number $lq_\theta$ greater than parallel wave number $k$ such that $\Upsilon = 0.5$, (ii) when the azimuthal wave number $lq_\theta$ is equal to the parallel wave number $k$ such that $\Upsilon = 1$, and (iii) for the azimuthal wave number $lq_\theta$ is less than parallel wave number $k$ such that $\Upsilon = 1.5$ for the non-planar (azimuthal electric field) cases, respectively, and one for the planar electric field case (iv) for the very small azimuthal wave number (so that $lq_\theta \cong 0$) in comparison to parallel wave number $k$ such that $\Upsilon = \infty$. It can be observed from Figures 1(a) and 1(b) that normalized Landau damping rate of the twisted ion acoustic wave $\gamma/\omega_r$ is least for $\Upsilon = 1$, while smaller for $\Upsilon = 1.5 > 1$ and larger for $\Upsilon = 0.5 < 1$ as compared with each other for the non-planar (azimuthal electric field) case. The physical reason of wave damping rate to be large for $\Upsilon = 0.5 < 1$ case seems to be that for large azimuthal wave number the more number of particles will take energy from the wave and the phenomenon wave particle interaction increases. Therefore, the damping of the wave for $\Upsilon = 0.5 < 1$ case is traced below than $\Upsilon = 1.5$ and $\Upsilon = 1$ cases. However, if we compare the wave damping rate of the twisted wave cases ($\Upsilon = 0.5$, 1, and 1.5) with the planar

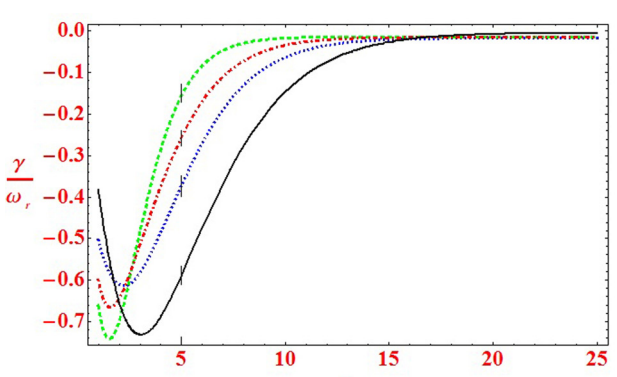


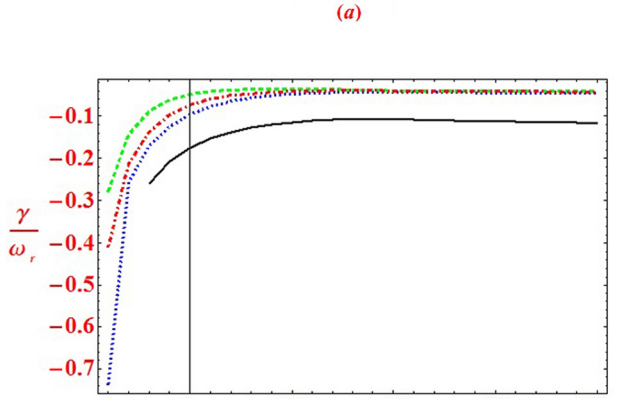


FIG. 1. **(a)** The plots of normalized weak Landau damping rate $\gamma/\omega_r$ obtained analytically described in Eqs. (31)–(33) are presented against the temperature ratio of electrons to ions $\beta = T_e/T_i$, for the twisted ion acoustic modes using different values of $\Upsilon = k/lq_\theta$, i.e., ($\Upsilon = 0.5$: Blue dotted curve), ($\Upsilon = 1$: Green dashed curve), and ($\Upsilon = 1.5$: Red dotted dashed curve) as well as for planar ion acoustic mode, i.e., $\Upsilon \to \infty$ (Black solid curve) are shown for kappa distributed electrons case, i.e., at $\kappa \to \infty$ and $k\lambda_{De} = 0.1$. **(b)** The exact numerical results are shown of normalized strong Landau damping rate $\gamma/\omega_r$ obtained from Eq. (21) by putting $\epsilon(\omega, k, lq_\theta) = 0$ against the temperature ratio of electrons to ions $\beta = T_e/T_i$, for the twisted ion acoustic modes using different values of $\Upsilon = k/lq_\theta$, i.e., ($\Upsilon = 0.5$: Blue dotted curve), ($\Upsilon = 1$: Green dashed curve), and ($\Upsilon = 1.5$: Red solid curve) as well as for planar ion acoustic mode, i.e., $\Upsilon \to \infty$ (Black solid curve) at $\kappa \to \infty$ and $k\lambda_{De} = 0.1$.

case ($\Upsilon = \infty$), the black planar curve appears below the twisted curves showing higher damping values for the planar mode in comparison to non-planar (twisted) ion acoustic mode.

Now we will study the comparison of our analytical and exact numerical results for twisted ion acoustic wave in non-thermal electrons plasmas. In Figure1(a), the curves obtained through analytical results show growing trend instead of damping about $\beta = 3$ which violates the physical interpretation of increasing damping rates of the ion acoustic wave at low values of temperature ratio of electron and ion. It happens as the weak damping approximation ($\xi_{zi}$, $\xi_{zi} \gg 1$ and $\xi_{\theta e}$, $\xi_{ze} \ll 1$) of the twisted ion acoustic wave has been used to expand the plasma dispersion function for obtaining analytical results and the numerical plot is shown in Figure 1(a). In order to encounter the weak damping approximation, the exact numerical results for strong damping rates of twisted ion acoustic modes are also reported in Figure 1(b) for the same values of $\Upsilon$. Now the growing trend of damping curves is almost removed at the values of temperature ratio less than $\beta = 3$ which agrees well with the increasing behavior of Landau damping phenomenon of twisted ion acoustic waves at low values of electron to ions temperature ratio.

In Figures 2(a) and 2(b), the analytical and exact numerical plots of normalized Landau damping rates $\gamma/\omega_r$ of the twisted ion acoustic waves against $\beta = T_e/T_i$ (the temperature ratio of electrons to ions) are presented for the kappa distributed electrons, i.e., $\kappa = 3$. We have shown the Landau damping rates of the twisted ion acoustic wave for three distinct values of $\Upsilon = k/lq_\theta$ (ratio of parallel to azimuthal wave number), i.e., (i) for $lq_\theta > k$ such that $\Upsilon = 0.5$, (ii) when $lq_\theta = k$ such that $\Upsilon = 1$, and (iii) for $lq_\theta < k$ such that $\Upsilon = 1.5$ for the non-planar (azimuthal electric field) cases, respectively, and one for the planar electric field case (iv) for the very small azimuthal wave number (so that $lq_\theta \cong 0$) in comparison to parallel wave number $k$ such that $\Upsilon \to \infty$. It is observed from figures that the Landau damping rate is larger at $\Upsilon = 0.5$, in comparison to $\Upsilon = 1.5$ and $\Upsilon = 1$. It is because of the presence of number of particles increases to take energy from the ion acoustic wave at $\Upsilon = 0.5$ in the energy spectrum. That is why blue dotted curve appears below the red dotted dashed and green dashed curves. But if we compare ($lq_\theta < k$ such that $\Upsilon = 1.5$ and $lq_\theta = k$ such that $\Upsilon = 1$) with each other, then the Landau damping rate of $\Upsilon = 1.5$ is larger as compared with $\Upsilon = 1$. It is due to the fact that the balancing of parallel and azimuthal wave numbers reduces the wave particle interaction phenomena. That is why green dotted curve is above the red dotted dashed curve. Now if we compare the planar case $\Upsilon \to \infty$ with the non-planar ones $\Upsilon = 0.5$, 1, and 1.5, then the damping of planar curve (shown by black solid curve) is again seen to be traced below the non-planar curves.

We compare twisted ion acoustic wave damping curves of both the analytical and exact numerical results for non-thermal electrons plasma. It is seen that the analytical curves show growing trend instead of damping near the values of $\beta = 5$ which is not in accordance to the physical interpretation of increasing damping rates at low value of $\beta$ which is defined in terms of electron to ion temperature ratio. This

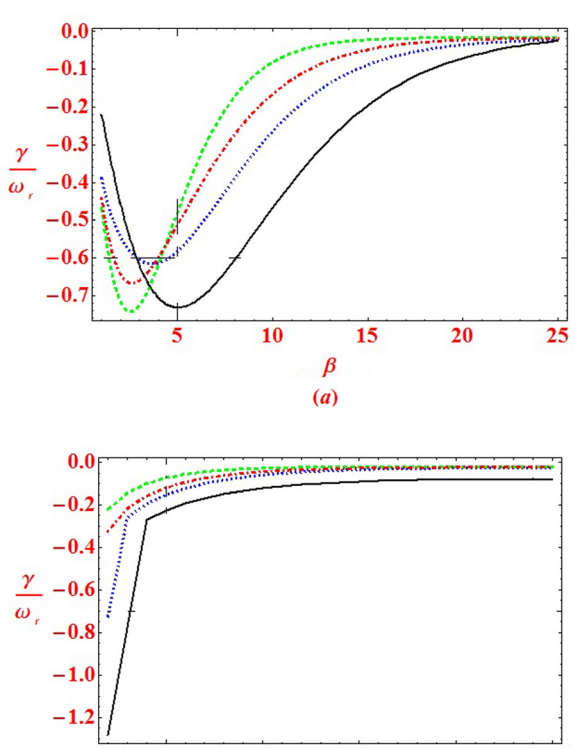


FIG. 2. **(a)** The plots of normalized weak Landau damping rate $\gamma/\omega_r$ obtained analytically described in Eqs. (31)–(33) are presented against the temperature ratio of electrons to ions $\beta = T_e/T_i$, for the twisted ion acoustic modes using different values of $\Upsilon = k/lq_\theta$, i.e., ($\Upsilon = 0.5$: Blue dotted curve), ($\Upsilon = 1$: Green dashed curve), and ($\Upsilon = 1.5$: Red dotted dashed curve) as well as for planar ion acoustic mode, i.e., $\Upsilon \to \infty$ (Black solid curve) are shown for Maxwellian distributed electrons case, i.e., at $\kappa = 3$ and $k\lambda_{De} = 0.1$. **(b)** The exact numerical results are shown of normalized strong Landau damping rate $\gamma/\omega_r$ obtained from Eq. (21) by putting $\epsilon(\omega, k, lq_\theta) = 0$ against the temperature ratio of electrons to ions $\beta = T_e/T_i$, for the twisted ion acoustic modes using different values of $\Upsilon = k/lq_\theta$, i.e., ($\Upsilon = 0.5$: Blue dotted curve), ($\Upsilon = 1$: Green dashed curve), and ($\Upsilon = 1.5$: Red solid curve) as well as for planar ion acoustic mode, i.e., $\Upsilon \to \infty$ (Black solid curve) at $\kappa = 3$ and $k\lambda_{De} = 0.1$.

behavior is the outcome of the weak damping approximation employed for obtaining analytical results shown in Figure 2(a) for the twisted ion acoustic wave. In order to show physically valid behavior throughout the curve, the exact numerical results of damping rates of twisted ion acoustic modes are also reported in Fig. 1(b) for the same values of $\Upsilon$. Now the growing trend of damping curves is removed for the less values of electrons to ions temperature ratio $\beta = 5$ and it agrees well with the physical explanation of the Landau damping rate of twisted ion acoustic wave in non-thermal electrons plasma at low values of $\beta$.

Figure 3 presents the exact numerical plots of normalized Landau damping rates $\gamma/\omega_r$ against the temperature ratio of electrons to ions, i.e., $\beta = T_e/T_i$ of the twisted ion acoustic waves having fixed kappa distributed electrons, i.e., $\kappa = 3$, and ratio of parallel to azimuthal wave number, i.e., $\Upsilon = 1$ for three distinct values of wave number which are normalized electron Debye length such that $k\lambda_{De} = 0.3$, $k\lambda_{De} = 0.6$, and $k\lambda_{De} = 0.9$. It is obvious that the damping rate of the twisted ion acoustic waves is high

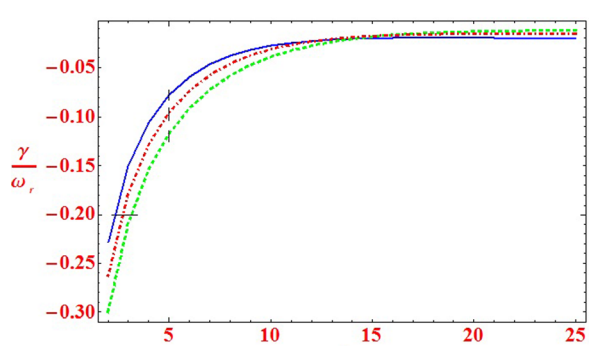


FIG. 3. The exact numerical results are shown of normalized strong Landau damping rate $\gamma/\omega_r$ obtained from Eq. (21) by putting $\epsilon(\omega, k, lq_\theta) = 0$ against the temperature ratio of electrons to ions $\beta = T_e/T_i$, for the twisted ion acoustic modes using different values of $k\lambda_{De}$, i.e., ($k\lambda_{De} = 0.9$: Green dashed curve), ($k\lambda_{De} = 0.6$: Red dotted dashed curve), and ($k\lambda_{De} = 0.3$: Blue solid curve) at $\kappa = 3$ and $\Upsilon = k/lq_\theta = 1$.

for $k\lambda_{De} = 0.9$, which is due to the fact that the damping rate of the wave increases as it wavelength approaches to the electron Debye length.

Finally, Figure 4 provides the comparison of Landau damping rates with Maxwellian ($\kappa \to \infty$) and non-Maxwellian or kappa distributed ($\kappa = 3$) electrons Vs the temperature ratio of electrons to ions, i.e., $\beta = T_e/T_i$ of the twisted ion acoustic waves. The purple dotted dashed curve is shown below the black solid line which clearly indicates that the Landau damping rate of purple curve (corresponds to kappa: $\kappa = 3$) is higher than black curve (i.e., $\kappa \to \infty$, containing Maxwellian distributed electrons). It reveals that the Lorentzian distributed superthermal electrons absorb more energy from the twisted ion acoustic wave as compare to Maxwellian distributed electrons case as they have more energetic electrons in the tail of energy spectrum. Therefore, Landau damping of the twisted ion acoustic wave is larger for the electrons following generalized Lorentzian or kappa distribution and smaller for the Maxwellian distributed electrons as shown in the figure.

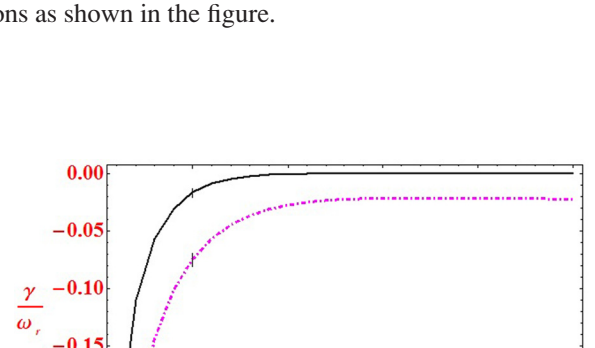


FIG. 4. The exact numerical results are shown of normalized strong Landau damping rate $\gamma/\omega_r$ obtained from Eq. (21) by putting $\epsilon(\omega, k, lq_\theta) = 0$ against the temperature ratio of electrons to ions $\beta = T_e/T_i$, for the twisted ion acoustic modes using different values of spectral indices $\kappa$, i.e., ($\kappa = 3$: Purple dotted dashed curve) and ($\kappa \to \infty$: Black solid curve) at $k\lambda_{De} = 0.1$ and $\Upsilon = k/lq_\theta = 1$.

## V. CONCLUSION

To conclude, we have studied the kinetic description of the damping rate Vs temperature ratio of the electrons to ions of the ion acoustic twisted wave in non-thermal kappa distributed electrons plasma. The twisted ion acoustic waves in electron-ion plasma are studied using the Vlasov-Poisson equation and the plasma dielectric function is derived in the presence of the orbital angular momentum (OAM) of the helical (non-planar or twisted) electric field perturbations with kappa distributed electrons and Maxwellian distributed ions. The perturbed distribution function and electric field are decomposed into Laguerre-Gaussian (LG) modes described in cylindrical coordinates. The analytical results for weak damping rates of the twisted and planar ion acoustic waves are obtained and plotted numerically as well. The exact numerical plots for strong damping effects of the twisted ion acoustic wave at low values of temperature ratio of electrons to ions are also investigated using the Newton Raphson method, where the weak damping wave theory fails to explain the Landau damping phenomenon properly.

Our results are applicable to laser plasma interactions and in space plasmas, where the helical electric field perturbations with non-thermal electrons and thermal ions plasmas can exist. The laser heating of plasmas has been investigated in many experiments and the Landau damping of ion acoustic waves in deuterium ($D^+$) plasma is studied at $T_e = 5T_i$.[37] A comparative study of ion acoustic wave damping is investigated by analytical as well as exact numerical approaches as shown in Fig. (8.18) of Ref. 38 against the temperature ratio of electron to ion, i.e., $T_e/T_i$. This figure clearly shows that strong ion acoustic wave damping effects appear when $T_e/T_i \simeq 1$, i.e., the electron temperature approaches the ion temperature, which can be studied through only the numerical approach. The electrostatic waves in Saturn's magnetosphere[39] are simulated by the particle in cell (PIC) scheme. In the case of ordinary electrons, the dispersion diagrams of ion acoustic wave are studied with ($T_e/T_i = 1$, 50, and 100), indicating that the range of temperature ratio of electron to ion (i.e., $T_e/T_i = 1 - 100$) and possible ratio of temperatures of hot ($T_h$) and cold electrons ($T_c$) to ions ($T_c/T_i = 2$, 10 and $T_h/T_i = 200$, 1000) are also discussed. In some space plasma regions, the ion temperature is reported higher in comparison to the electron temperature, i.e., $T_i/T_e > 1$. In the magnetotail, the qualitative investigations are made for the proton-electron plasma sheet and ion to electron temperature ratio $T_i/T_e$ is reported between 4 and 6.[40] In the solar wind termination shock,[41] the role of electrons is very important. The interaction of electrons and shock electric field caused the distribution of downstream electrons to be non-thermal (kappa). In conclusion, our present study holds for $T_i/T_e < 1$ which remains valid for studying twisted ion acoustic waves in nonthermal plasmas.

## APPENDIX: PROPERTIES OF LAGUERRE-GAUSSIAN (LG) MODE FUNCTION

- The Laguerre-Gaussian (LG) mode function $F_{pl}(r, z)$ is defined as[34]

$$F_{pl}(r,z) = C_{pl}X^{|l|}L_p^{|l|}(X)\exp(-X/2),$$

where $X = r^2/w^2(z)$ such that $w(z)$ is the beam waist. Here, integers $p$ and $l$ are the radial and angular mode numbers, while $\theta$ denotes the azimuthal angle.

We can define the normalization constants $C_{pl}$ and the associated Laguerre polynomials $L_p^{|l|}(X)$ by the following expressions:

$$C_{pl} = \sqrt{(l+p)!/4\pi p!},$$

and

$$L_p^{|l|}(X) = \exp(X)d^p/dX^p[X^{l+p}\exp(-X)]/p!X.$$

The orthogonality condition for the Laguerre-Gaussian (LG) modes is given by the equation

$$\langle F_{p'l'} \cdot |F_{pl}\rangle = \int_0^{2\pi} d\theta \int_0^{\infty} rdrF_{p'l'}F_{pl}\exp[i(l-l')\theta] = \delta_{pp'}\delta_{ll'}.$$


[1]J. H. Poynting, "The wave motion of a revolving shaft, and a suggestion as to the angular momentum in a beam of circularly polarised light," Proc. R. Soc. London **82**(557), 560–567 (1909).
[2]L. Allen, S. M. Barnett, and M. J. Padgett, *Optical Angular Momentum* (IOP Publishing, Bristol, UK, 2003).
[3]A. O. Barut, *Electrodynamics and Classical Theory of Fields and Particles* (Dover Publications, Inc., New York, NY, 1980).
[4]C. Cohen-Tannoudji, J. Dupont-Roc, and G. Grynberg, *Photons and Atoms: Introduction to Quantum Electrodynamics* (Wiley-Interscience, New York, NY, 1997).
[5]J. Schwinger, L. L. Deraad, Jr., K. A. Milton, and W. Tsai, *Classical Electrodynamics* (Perseus Books, Reading, MA, 1998).
[6]H. He, M. E. J. Friese, N. R. Heckenberg, and H. Rubinsztein-Dunlop, Phys. Rev. Lett. **75**, 826 (1995).
[7]C. Paterson, Phys. Rev. Lett. **94**, 153901 (2005).
[8]G. Molina-Terriza, J. P. Torres, and L. Torner, Nat. Phys. **3**, 305 (2007).
[9]B. Thide, H. Then, J. Sjoholm, K. Palmer, J. Bergman, T. D. Carozzi, Ya. N. Istomin, N. H. Ibragimov, and R. Khamitova, Phys. Rev. Lett. **99**, 087701 (2007); M. Harwit, Astrophys. J. **597**, 1266 (2003).
[10]B. Zolesi and L. R. Cander, *Ionospheric Prediction and Forecasting* (Springer Geophysics, 2014); J. A. Lee, J. Carini, A. Choi, R. Dillman, S. J. Griffin, S. Hanneman, C. Mamplata, and E. Stanton, Lunar Lander Conceptual Design, University of Virginia, 1989.
[11]S. Ali, J. R. Davies, and J. T. Mendonca, Phys. Rev. Lett. **105**, 035001 (2010).
[12]J. T. Mendonca and B. Thide, Europhys. Lett. **84**, 41001 (2008).
[13]J. T. Mendonca, S. Ali, and B. Thide, Phys. Plasmas **16**, 112103 (2009).
[14]P. W. Milonni and J. H. Eberly, *Laser Physics* (John Wiley and Sons, 2010).
[15]K. Sueda, N. M. G. Miyaji, and M. Nakatsuka, Opt. Express **12**(15), 3548–3553 (2004).
[16]L. Allen, M. W. Beijersbergen, R. J. C. Spreeuw, and J. P. Woerdman, Phys. Rev. A **45**, 8185 (1992).
[17]M. V. Khotyaintsev, V. N. Melnik, B. Thide, and O. O. Konovalenko, "Combination scattering by anisotropic Langmuir turbulence with application to solar radar experiments," Sol. Phys. **234**(1), 169–186 (2006); M. Khotyaintsev, "Radar probing of the Sun," Ph.D. thesis (Uppsala University, Uppsala, Sweden, 2006).
[18]M. Harwit, Astrophys. J. **597**, 1266 (2003).
[19]B. Thide, E. N. Sergreev, S. M. Grach, T. B. Leyser, and T. D. Carozzi, Phys. Rev. Lett. **95**(25), 255002 (2005).
[20]P. K. Shukla, B. Eliasson, and L. Stenflo, Phys. Rev. E **86**, 016403 (2012).
[21]P. K. Shukla, J. Geophys. Res.: Space Phys. **118**, 1–4 (2013).
[22]J. T. Mendonca, B. Thide, and H. Then, Phys. Rev. Lett. **102**, 185005 (2009).
[23]P. K. Shukla, Phys. Plasmas **19**, 083704 (2012).
[24]J. T. Mendonca, Plasma Phys. Controlled Fusion **54**, 124031 (2012).
[25]P. K. Shukla, Phys. Lett. A **376**, 2792–2794 (2012).
[26]T. B. Leyser, L. Norin, M. McCarrick, T. R. Pedersen, and B. Gustavsson, Phys. Rev. Lett. **102**, 065004 (2009).
[27]P. K. Shukla, Phys. Rev. E **87**, 015101 (2013).
[28]N. Yadav and R. P. Sharma, Sol. Phys. **289**, 1803–1814 (2014).
[29]J. T. Mendonca, Phys. Plasmas **19**, 112113 (2012).
[30]S. A. Khan, A. Rehman, and J. T. Mendonca, Phys. Plasmas **21**, 092109 (2014).
[31]K. Arshad and S. Mahmood, Phys. Plasmas **17**, 124501 (2010).
[32]K. Arshad, Z. Ehsan, S. A. Khan, and S. Mahmood, Phys. Plasmas **21**, 023704 (2014).
[33]K. Arshad, S. Mahmood, and A. M. Mirza, Phys. Plasmas **18**, 092115 (2011).
[34]K. Arshad, A. Rehman, and S. Mahmood, Phys. Plasmas **22**, 112114 (2015).
[35]A. F. Alexandrov, L. S. Bogdankevich, and A. A. Rukhadze, *Principles of Plasma Electrodynamics* (Springer-Verlag. Berlin, Heidelberg, New York, Tokio, 1984).
[36]A. Iserles, *A First Course in the Numerical Analysis of Differential Equations*, 2nd ed. (Cambridge University Press, 2009).
[37]H. Hora, *Laser Plasmas and Nuclear Energy* (Plenum Press, New York, 1975).
[38]D. A. Gurnett and A. Bhattacharjee, *Introduction to Plasma Physics: With Space and Laboratory Applications* (Cambridge Press, 2005).
[39]L. G. Pedraza, Particle in Cell Simulations of Electrostatic Waves in Saturn's Magnetosphere, 2012.
[40]D. Schriver, M. Ashour-Abdalla, and R. L. Richard, J. Geophys. Res. **103**, 14879, doi:10.1029/98JA00017 (1998).
[41]H. J. Fahr, J. D. Richardson, and D. Verscharen, Astron. Astrophys. **579**, A18 (2015).